

# Supplemental Material: Quenching of excited rovibrational states of $\text{H}_2^+$ in an external magnetic field

Jean-Philippe Karr<sup>1,2</sup>

<sup>1</sup>*Laboratoire Kastler Brossel, Sorbonne Université, CNRS,  
ENS-PSL Research University, Collège de France  
4 place Jussieu, F-75005 Paris, France*

<sup>2</sup>*Université d'Evry-Val d'Essonne, Université Paris-Saclay,  
Boulevard François Mitterrand, F-91000 Evry, France*

The two-photon matrix elements  $Q_s$ ,  $Q_v$ , and  $Q_t$  defined in Eqs. (21-23), in atomic units (that is  $(ea_0)^2/E_h = 4\pi\epsilon_0 a_0^3$ ) where  $a_0$  is the Bohr radius and  $E_h$  the Hartree energy), are given in the following Tables for  $L \rightarrow L' = L - 2$  ( $\Delta v = v - v' = 0, 1, 2$ , Tables I-III),  $L \rightarrow L' = L$  ( $\Delta v = 1, 2$ , Tables IV-V), and  $L \rightarrow L' = L + 2$  transitions ( $\Delta v = 1, 2$ , Tables VI-VII).

It is worth noting that for  $L \rightarrow L$  transitions, the rank 1 component  $Q_v$  is comparatively small and may safely be ignored for calculating decay rates at the 4-digit accuracy level.

TABLE I: Two-photon matrix elements  $Q_t$  in atomic units, with  $L' = L - 2$  and  $v' = v$ .

$L/v$	0	1	2	3	4	5	6	7	8	9	10	11	12
2	2.6840	3.8218	5.3437	7.3899	10.163	13.962	19.240	26.705	37.504	53.572	78.347	118.33	186.85
3	2.0986	2.9873	4.1762	5.7752	7.9431	10.915	15.047	20.896	29.368	41.992	61.494	93.049	
4	1.9704	2.8034	3.9182	5.4183	7.4535	10.246	14.132	19.643	27.637	39.578	58.077	88.125	
5	1.9316	2.7466	3.8376	5.3068	7.3018	10.042	13.863	19.290	27.182	39.006	57.398		
6	1.9313	2.7440	3.8328	5.3003	7.2954	10.040	13.874	19.333	27.297	39.275	58.000		
7	1.9542	2.7744	3.8740	5.3575	7.3776	10.162	14.060	19.628	27.780	40.101			
8	1.9946	2.8292	3.9493	5.4626	7.5267	10.378	14.382	20.120	28.562	41.393			
9	2.0498	2.9050	4.0540	5.6089	7.7341	10.678	14.825	20.794	29.622				
10	2.1189	3.0003	4.1862	5.7940	7.9970	11.058	15.387	21.649	30.967				
11	2.2015	3.1148	4.3457	6.0180	8.3159	11.520	16.072	22.694					
12	2.2979	3.2490	4.5332	6.2824	8.6937	12.070	16.891	23.951					
13	2.4088	3.4039	4.7504	6.5899	9.1351	12.715	17.858						
14	2.5350	3.5808	4.9996	6.9444	9.6465	13.468	18.994						
15	2.6777	3.7817	5.2839	7.3506	10.236	14.341							
16	2.8383	4.0088	5.6069	7.8149	10.914	15.354							
17	3.0185	4.2649	5.9730	8.3445	11.694	16.528							
18	3.2205	4.5534	6.3878	8.9488	12.590								
19	3.4465	4.8780	6.8578	9.6387	13.624								
20	3.6993	5.2435	7.3908	10.428									
21	3.9823	5.6554	7.9965	11.334									
22	4.2993	6.1203	8.6862										
23	4.6548	6.6462	9.4744										
24	5.0544	7.2428											
25	5.5043	7.9218											
26	6.0124												
27	6.5880												





TABLE IV: Two-photon matrix elements  $Q_s$  (first line)  $Q_v$  (second line) and  $Q_t$  (third line) in atomic units, with  $L' = L$  and  $v' = v - 1$ .

$L/v$	1	2	3	4	5	6	7	8	9	10	11	12
0	-0.83797	-1.4013	-2.0514	-2.8653	-3.9272	-5.3537	-7.3199	-10.102	-14.153	-20.255	-29.827	-45.641
1	-0.84102	-1.4067	-2.0598	-2.8778	-3.9456	-5.3805	-7.3596	-10.162	-14.245	-20.401	-30.070	-46.067
1	0.00004	0.00009	0.00016	0.00028	0.00047	0.00079	0.00134	0.00233	0.00415	0.00772	0.01520	0.03240
1	0.73131	1.3010	2.0122	2.9502	4.2184	5.9648	8.4139	11.920	17.068	24.861	37.131	57.453
2	-0.84714	-1.4175	-2.0766	-2.9029	-3.9824	-5.4346	-7.4397	-10.282	-14.431	-20.697	-30.562	-46.933
2	0.00008	0.00016	0.00029	0.00049	0.00083	0.00140	0.00237	0.00411	0.00734	0.01369	0.02708	0.05797
2	0.62401	1.1104	1.7178	2.5194	3.6038	5.0984	7.1964	10.204	14.624	21.329	31.910	49.487
3	-0.85639	-1.4339	-2.1020	-2.9409	-4.0383	-5.5167	-7.5615	-10.466	-14.715	-21.150	-31.317	
3	0.00011	0.00023	0.00041	0.00071	0.00120	0.00202	0.00345	0.00598	0.01073	0.02009	0.03993	
3	0.61153	1.0885	1.6846	2.4719	3.5382	5.0095	7.0777	10.048	14.423	21.076	31.612	
4	-0.86884	-1.4560	-2.1365	-2.9922	-4.1139	-5.6281	-7.7270	-10.716	-15.103	-21.771	-32.358	
4	0.00015	0.00030	0.00055	0.00095	0.00160	0.00270	0.00461	0.00804	0.01447	0.02724	0.05454	
4	0.61508	1.0953	1.6960	2.4903	3.5676	5.0564	7.1534	10.172	14.631	21.437	32.266	
5	-0.88459	-1.4839	-2.1801	-3.0575	-4.2102	-5.7702	-7.9389	-11.038	-15.603	-22.577		
5	0.00019	0.00039	0.00070	0.00120	0.00204	0.00345	0.00590	0.01034	0.01871	0.03548		
5	0.62567	1.1147	1.7273	2.5385	3.6405	5.1666	7.3214	10.432	15.045	22.119		
6	-0.90379	-1.5181	-2.2335	-3.1376	-4.3286	-5.9455	-8.2009	-11.437	-16.227	-23.588		
6	0.00023	0.00047	0.00086	0.00148	0.00252	0.00428	0.00737	0.01297	0.02364	0.04522		
6	0.64111	1.1429	1.7725	2.6077	3.7446	5.3231	7.5586	10.798	15.623	23.064		
7	-0.92659	-1.5587	-2.2972	-3.2333	-4.4706	-6.1565	-8.5178	-11.922	-16.990			
7	0.00027	0.00057	0.00104	0.00180	0.00307	0.00524	0.00906	0.01605	0.02948			
7	0.66071	1.1788	1.8300	2.6956	3.8769	5.5219	7.8599	11.262	16.358			
8	-0.95322	-1.6063	-2.3719	-3.3460	-4.6384	-6.4067	-8.8953	-12.503	-17.910			
8	0.00033	0.00068	0.00124	0.00216	0.00370	0.00634	0.01103	0.01969	0.03653			
8	0.68435	1.2221	1.8994	2.8020	4.0373	5.7635	8.2273	11.831	17.263			
9	-0.98391	-1.6612	-2.4586	-3.4771	-4.8344	-6.7004	-9.3409	-13.193				
9	0.00038	0.00081	0.00147	0.00257	0.00443	0.00763	0.01337	0.02407				
9	0.71209	1.2730	1.9812	2.9276	4.2273	6.0508	8.6659	12.514				
10	-1.0190	-1.7242	-2.5582	-3.6285	-5.0617	-7.0427	-9.8637	-14.010				
10	0.00045	0.00095	0.00174	0.00305	0.00527	0.00916	0.01617	0.02941				
10	0.74414	1.3319	2.0761	3.0740	4.4495	6.3882	9.1841	13.327				
11	-1.0587	-1.7959	-2.6721	-3.8023	-5.3239	-7.4402	-10.475					
11	0.00053	0.00111	0.00205	0.00361	0.00627	0.01097	0.01955					
11	0.78083	1.3995	2.1854	3.2430	4.7073	6.7818	9.7926					
12	-1.1036	-1.8772	-2.8017	-4.0010	-5.6257	-7.9007	-11.189					
12	0.00061	0.00130	0.00240	0.00426	0.00746	0.01316	0.02370					
12	0.82254	1.4767	2.3105	3.4373	5.0051	7.2394	10.505					
13	-1.1541	-1.9690	-2.9489	-4.2280	-5.9724	-8.4340						
13	0.00071	0.00152	0.00282	0.00503	0.00888	0.01582						
13	0.86974	1.5642	2.4532	3.6600	5.3484	7.7705						
14	-1.2108	-2.0724	-3.1156	-4.4868	-6.3709	-9.0520						
14	0.00083	0.00177	0.00331	0.00595	0.01060	0.01907						
14	0.92301	1.6634	2.6155	3.9148	5.7438	8.3873						
15	-1.2742	-2.1890	-3.3046	-4.7821	-6.8291							
15	0.00096	0.00207	0.00389	0.00705	0.01268							
15	0.98302	1.7757	2.8001	4.2063	6.1996							
16	-1.3453	-2.3203	-3.5189	-5.1195	-7.3575							
16	0.00112	0.00242	0.00459	0.00838	0.01523							
16	1.0506	1.9027	3.0101	4.5402	6.7259							
17	-1.4250	-2.4683	-3.7622	-5.5058	-7.9684							
17	0.00130	0.00283	0.00542	0.00999	0.01838							
17	1.1266	2.0463	3.2492	4.9233	7.3357							
18	-1.5142	-2.6353	-4.0388	-5.9492								
18	0.00151	0.00332	0.00641	0.01196								
18	1.2122	2.2090	3.5219	5.3640								
19	-1.6143	-2.8240	-4.3544	-6.4603								
19	0.00177	0.00391	0.00762	0.01438								
19	1.3087	2.3935	3.8337	5.8729								
20	-1.7269	-3.0380	-4.7155									

(continued on next page)



TABLE V: Same as Table IV, with  $v' = v - 2$ .

$L/v$	2	3	4	5	6	7	8	9	10	11	12
0	-0.03562	-0.08270	-0.15560	-0.26641	-0.43284	-0.68172	-1.0547	-1.6186	-2.4838	-3.8426	-6.0497
1	-0.03587	-0.08328	-0.15668	-0.26825	-0.43585	-0.68654	-1.0624	-1.6308	-2.5035	-3.8751	-6.1053
1	0.00003	0.00006	0.00012	0.00023	0.00041	0.00073	0.00131	0.00240	0.00453	0.00895	0.01885
1	0.08291	0.17403	0.30084	0.47932	0.73230	1.0941	1.6179	2.3884	3.5465	5.3373	8.2150
2	-0.03639	-0.08444	-0.15884	-0.27195	-0.44191	-0.69626	-1.0779	-1.6554	-2.5433	-3.9410	-6.2183
2	0.00005	0.00011	0.00022	0.00040	0.00072	0.00129	0.00232	0.00425	0.00804	0.01592	0.03367
2	0.07078	0.14860	0.25698	0.40961	0.62610	0.93596	1.3849	2.0461	3.0412	4.5827	7.0652
3	-0.03717	-0.08621	-0.16213	-0.27758	-0.45113	-0.71106	-1.1014	-1.6931	-2.6042	-4.0419	
3	0.00007	0.00016	0.00031	0.00058	0.00105	0.00188	0.00338	0.00621	0.01179	0.02346	
3	0.06941	0.14579	0.25226	0.40233	0.61542	0.92077	1.3638	2.0173	3.0029	4.5335	
4	-0.03824	-0.08862	-0.16660	-0.28522	-0.46367	-0.73121	-1.1336	-1.7445	-2.6876	-4.1805	
4	0.00009	0.00021	0.00042	0.00078	0.00140	0.00251	0.00454	0.00837	0.01597	0.03197	
4	0.06987	0.14687	0.25430	0.40593	0.62152	0.93093	1.3807	2.0456	3.0511	4.6182	
5	-0.03960	-0.09169	-0.17232	-0.29501	-0.47975	-0.75708	-1.1749	-1.8108	-2.7955		
5	0.00011	0.00026	0.00053	0.00099	0.00179	0.00322	0.00584	0.01082	0.02077		
5	0.07116	0.14969	0.25944	0.41455	0.63549	0.95320	1.4161	2.1024	3.1438		
6	-0.04128	-0.09549	-0.17938	-0.30711	-0.49965	-0.78915	-1.2263	-1.8935	-2.9305		
6	0.00013	0.00033	0.00065	0.00123	0.00223	0.00402	0.00733	0.01367	0.02642		
6	0.07302	0.15377	0.26679	0.42684	0.65527	0.98456	1.4657	2.1814	3.2722		
7	-0.04330	-0.10007	-0.18790	-0.32173	-0.52373	-0.82805	-1.2888	-1.9944			
7	0.00016	0.00040	0.00080	0.00149	0.00273	0.00495	0.00907	0.01703			
7	0.07540	0.15895	0.27613	0.44244	0.68039	1.0244	1.5287	2.2819			
8	-0.04569	-0.10550	-0.19802	-0.33912	-0.55243	-0.87454	-1.3637	-2.1159			
8	0.00019	0.00047	0.00096	0.00180	0.00331	0.00603	0.01113	0.02107			
8	0.07827	0.16522	0.28746	0.46138	0.71093	1.0729	1.6056	2.4051			
9	-0.04851	-0.11187	-0.20991	-0.35959	-0.58630	-0.92957	-1.4527				
9	0.00023	0.00056	0.00114	0.00216	0.00399	0.00732	0.01360				
9	0.08167	0.17264	0.30087	0.48385	0.74725	1.1307	1.6977				
10	-0.05178	-0.11929	-0.22378	-0.38352	-0.62600	-0.99430	-1.5580				
10	0.00027	0.00067	0.00136	0.00258	0.00479	0.00885	0.01661				
10	0.08561	0.18129	0.31655	-0.51017	0.78993	1.1990	1.8068				
11	-0.05556	-0.12789	-0.23988	-0.41135	-0.67233	-1.0702					
11	0.00032	0.00079	0.00161	0.00308	0.00575	0.01072					
11	0.09017	0.19128	0.33470	0.54077	0.83972	1.2790					
12	-0.05992	-0.13780	-0.25849	-0.44363	-0.72627	-1.1589					
12	0.00038	0.00093	0.00191	0.00367	0.00691	0.01299					
12	0.09539	0.20277	0.35564	0.57616	0.89757	1.3724					
13	-0.06492	-0.14922	-0.27997	-0.48101	-0.78899						
13	0.00044	0.00109	0.00226	0.00438	0.00831						
13	0.10135	0.21592	0.37969	0.61699	0.96465						
14	-0.07067	-0.16234	-0.30473	-0.52427	-0.86194						
14	0.00052	0.00129	0.00268	0.00524	0.01003						
14	0.10813	0.23095	0.40728	0.66405	1.0424						
15	-0.07725	-0.17742	-0.33328	-0.57436							
15	0.00061	0.00152	0.00319	0.00629							
15	0.11586	0.24811	0.43892	0.71831							
16	-0.08478	-0.19474	-0.36621	-0.63243							
16	0.00071	0.00180	0.00380	0.00757							
16	0.12464	0.26771	0.47523	0.78091							
17	-0.09342	-0.21466	-0.40425	-0.69990							
17	0.00084	0.00213	0.00455	0.00915							
17	0.13462	0.29010	0.51692								
18	-0.10333	-0.23760	-0.44828								
18	0.00099	0.00254	0.00546								
18	0.14599	0.31571	0.56491								
19	-0.11471	-0.26407	-0.49938								
19	0.00117	0.00303	0.00659								
19	0.15895	0.34506	0.62028								
20	-0.12780	-0.29469									
20	0.00139	0.00363									

(continued on next page)







# Stark quenching of rovibrational states of $\text{H}_2^+$ due to motion in a magnetic field

Jean-Philippe Karr

*Laboratoire Kastler Brossel,  
Sorbonne Université, CNRS,*

*ENS-PSL Research University, Collège de France*

*4 place Jussieu, F-75005 Paris, France and*

*Université d'Evry-Val d'Essonne, Université Paris-Saclay,  
Boulevard François Mitterrand, F-91000 Evry, France*

The motional electric field experienced by an  $\text{H}_2^+$  ion moving in a magnetic field induces an electric dipole, so that one-photon dipole transitions between rovibrational states become allowed. Field-induced spontaneous decay rates are calculated for a wide range of states. For an ion stored in a high-field ( $B \sim 10$  T) Penning trap, it is shown that the lifetimes of excited rovibrational states can be shortened by typically 1-3 orders of magnitude by placing the ion in a large cyclotron orbit. This can greatly facilitate recently proposed [E. G. Myers, Phys. Rev. A **98**, 010101 (2018)] high-precision spectroscopic measurements on  $\text{H}_2^+$  and its antimatter counterpart for tests of *CPT* symmetry.

## Introduction

The hydrogen molecular ions,  $\text{H}_2^+$  and its isotopes ( $\text{HD}^+$ ,  $\text{D}_2^+$ ) have long since been identified as a highly promising system for fundamental physics tests. High-precision spectroscopy of rovibrational transitions can be used to determine the proton-electron and deuteron-electron mass ratios [1, 2] and probe their possible time variation [3–5]. Furthermore, measuring an appropriate set of transitions in  $\text{H}_2^+$  and  $\text{HD}^+$  would allow a determination of the proton and deuteron charge radii and the Rydberg constant [6] and thus may contribute to resolving the existing discrepancies on their values [7–11]. Spectroscopy of  $\text{H}_2^+$  compared with its antimatter counterpart  $\bar{\text{H}}_2^-$  was recently proposed for improved tests of *CPT* symmetry [12].

Theoretical predictions of rovibrational transition frequencies have surpassed the  $10^{-11}$  accuracy level [13] which already allows for an improved determination of mass ratios [14, 15]. In  $\text{HD}^+$ , experiments with ultracold trapped ions have reached a precision of  $10^{-9}$  [16, 17] and more recently  $5 \times 10^{-10}$  [18]. Studies on  $\text{H}_2^+$  [19–23] have been so far performed by different techniques yielding lower accuracies. The main obstacle faced by ultrahigh-resolution spectroscopy of trapped  $\text{H}_2^+$  (or  $\bar{\text{H}}_2^-$ ) is quantum state preparation, due to the fact that, unlike in the heteronuclear  $\text{HD}^+$ , rovibrational transitions are not dipole-allowed. As a result, rovibrational states of vibration quantum number  $v \geq 1$  have very long lifetimes typically of the order of 10 days [24, 25]. It would take several months for an ion produced in e.g.  $v = 10$  to decay down to  $v = 0$ . Pure rotational transitions for lower values of rotational quantum number  $L$  are even slower, the rotational levels of  $v = 0$  with  $L < 8$  having lifetimes greater than one year, for example. In addition, optical pumping methods for cooling the internal degrees of freedom [26] are not available. One solution [27] consists in creating the ions directly in the desired rovibrational state by state-selective multiphoton ionization (REMPI) of  $\text{H}_2$  [28, 29]. However, no selective production scheme is available for antimatter  $\bar{\text{H}}_2^-$  ions [12]. Rovibrational cooling by cold He buffer gas has also been proposed [30] but is again not well suited for antimatter ions.

In this paper, we study another rovibrational relaxation process relevant for experiments performed in a Penning trap, first proposed in [12]. The idea is to exploit the motional electric field experienced by an ion as it moves in a magnetic field. This electric field polarizes the ion [31] making one-photon ro-vibrational decay allowed. The Stark quenching process is much less efficient in  $\text{H}_2^+$  as e.g. for the 2S state in hydrogen [32] because the mixing of  $1s\sigma_g$  rovibrational states induced by the electric field occurs with excited electronic states and is very weak. Nevertheless, our results show that rovibrational decay can typically be accelerated by at least one order of magnitude in a high-field ( $B \sim 10$  T) Penning trap.

In the following, we present the calculation of decay rates for a wide range of rovibrational states. The paper is structured as follows : the theoretical expression of the decay rate is derived in Sec. I. The numerical method is described in Sec. II. Results are presented in Sec. III, and their experimental implications briefly discussed.

## I. THEORY

### A. Motional electric field

We consider an  $\text{H}_2^+$  ion in a Penning trap with a uniform magnetic field  $\mathbf{B}_0$  along the  $z$  axis, placed in a cyclotron orbit of radius  $r_c$ . The ion's velocity is

$$\mathbf{v}(t) = \frac{qB_0 r_c}{m} [\sin(\omega_c t) \mathbf{e}_x + \cos(\omega_c t) \mathbf{e}_y] \quad (1)$$

where  $\omega_c = qB_0/m$  is the cyclotron frequency. The moving ion experiences a motional electric field

$$\mathbf{E}_0(t) = \mathbf{v}(t) \times \mathbf{B}_0 = E_0 [\cos(\omega_c t) \mathbf{e}_x - \sin(\omega_c t) \mathbf{e}_y] \quad (2)$$

with  $E_0 = qB_0^2 r_c/m$ . This electric field can be expressed in terms of the standard polarizations

$$\boldsymbol{\epsilon}_{\pm 1} = \mp \frac{1}{\sqrt{2}} (\mathbf{e}_x \pm i \mathbf{e}_y). \quad (3)$$

One gets :

$$\mathbf{E}_0(t) = \frac{E_0}{\sqrt{2}} (e^{-i\omega_c t} \boldsymbol{\epsilon}_{-1} + h.c.). \quad (4)$$

Decay induced by the field  $\mathbf{E}_0(t)$  can be understood as a two-photon process whereby a "cyclotron" photon of energy  $\hbar\omega_c$  is emitted (or absorbed) and another is spontaneously emitted. Since the cyclotron frequency is very small with respect to rovibrational transition frequencies in  $\text{H}_2^+$ , one may approximate  $\mathbf{E}_0(t)$  by a static field

$$\mathbf{E}_0 = \frac{E_0}{\sqrt{2}} (\boldsymbol{\epsilon}_{-1} - \boldsymbol{\epsilon}_1). \quad (5)$$

### B. Dipole matrix elements

A ro-vibrational state  $(v, L)$  of  $\text{H}_2^+$  supported by the ground ( $1s\sigma_g$ ) electronic curve will be mixed by the motional electric field with states of opposite parity supported by excited electronic curves. At the first order of perturbation theory, the perturbed wavefunction may be written as

$$|\psi_{v,L,M}^{(1)}\rangle = |\psi_{v,L,M}\rangle + \frac{1}{E_{v,L} - H} \mathbf{d} \cdot \mathbf{E}_0 |\psi_{v,L,M}\rangle \quad (6)$$

As a result, one-photon transitions between ro-vibrational states become dipole-allowed. Keeping only leading-order terms, the transition dipole moment is

$$\begin{aligned} \langle \psi_{v',L',M'}^{(1)} | \mathbf{d} \cdot \boldsymbol{\epsilon} | \psi_{v,L,M}^{(1)} \rangle &= E_0 \left( \langle \psi_{v',L',M'} | \mathbf{d} \cdot \boldsymbol{\epsilon} \frac{1}{E_{v,L} - H} \mathbf{d} \cdot \boldsymbol{\epsilon}_0 | \psi_{v,L,M} \rangle \right. \\ &\quad \left. + \langle \psi_{v',L',M'} | \mathbf{d} \cdot \boldsymbol{\epsilon}_0 \frac{1}{E_{v',L'} - H} \mathbf{d} \cdot \boldsymbol{\epsilon} | \psi_{v,L,M} \rangle \right) \end{aligned} \quad (7)$$

where  $\boldsymbol{\epsilon}_0 = (\boldsymbol{\epsilon}_{-1} - \boldsymbol{\epsilon}_1)/\sqrt{2}$ . This can be written in terms of the two-photon transition operator  $Q_{\boldsymbol{\epsilon}_1 \boldsymbol{\epsilon}_2}(\omega_1, \omega_2)$  [33, 34] :

$$\langle \psi_{v',L',M'}^{(1)} | \mathbf{d} \cdot \boldsymbol{\epsilon} | \psi_{v,L,M}^{(1)} \rangle = E_0 \langle \psi_{v',L',M'} | Q_{\boldsymbol{\epsilon}_0 \boldsymbol{\epsilon}}(0, \omega) | \psi_{v,L,M} \rangle, \quad (8)$$

where  $\hbar\omega = E_{v,L} - E_{v',L'}$ , and

$$Q_{\boldsymbol{\epsilon}_1 \boldsymbol{\epsilon}_2}(\omega_1, \omega_2) = Q_{\boldsymbol{\epsilon}_2 \boldsymbol{\epsilon}_1}(\omega_1) + Q_{\boldsymbol{\epsilon}_1 \boldsymbol{\epsilon}_2}(\omega_2), \quad (9)$$

$$Q_{\boldsymbol{\epsilon}_2 \boldsymbol{\epsilon}_1}(\omega_1) = \mathbf{d} \cdot \boldsymbol{\epsilon}_2 \frac{1}{E_{v,L} - \hbar\omega_1 - H} \mathbf{d} \cdot \boldsymbol{\epsilon}_1 \quad (10)$$

### C. Properties of the two-photon transition operator

Since this operator couples twice the vector operator  $\mathbf{d}$ , it may be written as a sum of operators of rank 0, 1 and 2. Furthermore, one can decompose it into its symmetrical and antisymmetrical parts [33]

$$Q_{\epsilon_1\epsilon_2}(\omega_1, \omega_2) = Q_{\epsilon_1\epsilon_2}^S(\omega_1, \omega_2) + Q_{\epsilon_1\epsilon_2}^A(\omega_1, \omega_2), \quad (11)$$

$$Q_{\epsilon_1\epsilon_2}^S(\omega_1, \omega_2) = \frac{1}{2}(Q_{\epsilon_1\epsilon_2}(\omega_1, \omega_2) + Q_{\epsilon_2\epsilon_1}(\omega_1, \omega_2)) \quad (12)$$

$$Q_{\epsilon_1\epsilon_2}^A(\omega_1, \omega_2) = \frac{1}{2}(Q_{\epsilon_1\epsilon_2}(\omega_1, \omega_2) - Q_{\epsilon_2\epsilon_1}(\omega_1, \omega_2)). \quad (13)$$

Then  $Q_{\epsilon_1\epsilon_2}^S(\omega_1, \omega_2)$  is decomposed into operators of ranks 0 and 2, while  $Q_{\epsilon_1\epsilon_2}^A(\omega_1, \omega_2)$  is of rank 1.

Selection rules for Stark-induced decay are thus identical to those of two-photon transitions [35], i.e.  $\Delta L = 0, \pm 2$  for rovibrational transitions within the  $1s\sigma_g$  electronic state.  $L = 0 \rightarrow L' = 0$  transitions only involve the scalar component of the two-photon operator, while  $L \rightarrow L \pm 2$  transitions only involve the rank 2 component. The  $L \rightarrow L$  transitions with  $L \geq 1$  are the most complicated cases, involving all three terms (rank 0, 1 and 2).

We define the scalar ( $Q^{(0)}$ ) and tensor ( $Q^{(2)}$ ) operators appearing in the decomposition of  $Q_{\epsilon_1\epsilon_2}^S$  by the relationship

$$Q_{00}^S = Q_0^{(0)} + Q_0^{(2)} \quad (14)$$

The required  $Q_{q_1q_2}^S$  components can then be expressed in terms of irreducible components  $Q_q^{(0)}$ ,  $Q_q^{(2)}$ . One obtains [5]

$$Q_{\pm 1\pm 1}^S = \sqrt{\frac{3}{2}}Q_{\pm 2}^{(2)} \quad (15)$$

$$Q_{\pm 10}^S = \frac{\sqrt{3}}{2}Q_{\pm 1}^{(2)} \quad (16)$$

$$Q_{\pm 1\mp 1}^S = -Q_0^{(0)} + \frac{1}{2}Q_0^{(2)} \quad (17)$$

Similarly, for the antisymmetrical part  $Q_{\epsilon_1\epsilon_2}^A$  we define the vector operator  $Q^{(1)}$  by the relationship

$$Q_{-10}^A = Q_{-1}^{(1)} \quad (18)$$

and the  $Q_{q_1q_2}^A$  components can be expressed in terms of irreducible components  $Q_q^{(1)}$  [33]

$$Q_{\pm 10}^A = \mp Q_{\pm 1}^{(1)} \quad (19)$$

$$Q_{\pm 1\mp 1}^A = \mp Q_0^{(1)} \quad (20)$$

Finally, we set

$$Q_s = \frac{\langle v'L' || Q^{(0)} || vL \rangle}{\sqrt{2L'+1}} \quad (21)$$

$$Q_v = \frac{\langle v'L' || Q^{(1)} || vL \rangle}{\sqrt{2L'+1}} \quad (22)$$

$$Q_t = \frac{\langle v'L' || Q^{(2)} || vL \rangle}{\sqrt{2L'+1}}. \quad (23)$$

### D. Decay rates

The decay rate (or Einstein coefficient  $A$ ) of a given state  $(v, L, M)$  associated with a transition towards a state  $(v', L')$  (in  $\text{s}^{-1}$ ) is given by

$$A_{v,L,M,v',L'} = \frac{2\omega^3}{3\epsilon_0\hbar c^3} \sum_{M',\epsilon} |\langle \psi_{v'L'M'} | \mathbf{d} \cdot \boldsymbol{\epsilon} | \psi_{v,L,M} \rangle|^2 \quad (24)$$

In the usual case of spontaneous emission in an isotropic environment, the decay rate does not depend on  $M$ , but here anisotropy arises from the fact that the electric field  $\mathbf{E}_0$  is polarized perpendicularly to the  $z$  axis.

In the simplest case  $L = L' = 0$  we get

$$A_{v,L=0,M=0,v',L'=0} = \frac{2\omega^3}{3\epsilon_0 hc^3} E_0^2 Q_s^2. \quad (25)$$

For  $L' = L \pm 2$  :

$$\begin{aligned} A_{v,L,M,v',L'} &= \frac{2\omega^3}{3\epsilon_0 hc^3} \frac{E_0^2}{2} \sum_{M',q} \left( |\langle v'L'M' | Q_{-1q}^S(0,\omega) | vLM \rangle|^2 + |\langle v'L'M' | Q_{1q}^S(0,\omega) | vLM \rangle|^2 \right) \\ &= \frac{\omega^3}{3\epsilon_0 hc^3} E_0^2 \left\{ \frac{3}{2} |\langle v'L'M+2 | Q_2^{(2)} | vLM \rangle|^2 + \frac{3}{2} |\langle v'L'M-2 | Q_{-2}^{(2)} | vLM \rangle|^2 \right. \\ &\quad \left. + \frac{3}{4} |\langle v'L'M+1 | Q_1^{(2)} | vLM \rangle|^2 + \frac{3}{4} |\langle v'L'M-1 | Q_{-1}^{(2)} | vLM \rangle|^2 + \frac{1}{2} |\langle v'L'M | Q_0^{(2)} | vLM \rangle|^2 \right\} \\ &= \frac{\omega^3}{3\epsilon_0 hc^3} E_0^2 \left\{ \frac{3}{2} |\langle LM22 | L'M+2 \rangle|^2 + \frac{3}{2} |\langle LM2-2 | L'M-2 \rangle|^2 \right. \\ &\quad \left. + \frac{3}{4} |\langle LM21 | L'M+1 \rangle|^2 + \frac{3}{4} |\langle LM2-1 | L'M-1 \rangle|^2 + \frac{1}{2} |\langle LM20 | L'M \rangle|^2 \right\} Q_t^2 \end{aligned} \quad (26)$$

One can show that the averaged decay rate  $\bar{A}_{v,L,v',L'} = \left( \sum_{M=-L}^L A_{v,L,M,v',L'} \right) / (2L+1)$  is

$$\bar{A}_{v,L,v',L'} = \frac{\omega^3}{3\epsilon_0 hc^3} E_0^2 Q_t^2 \frac{2L'+1}{2L+1}. \quad (27)$$

Finally, for  $L' = L \geq 1$  the spontaneous emission rate is

$$\begin{aligned} A_{v,L,M,v',L} &= \frac{2\omega^3}{3\epsilon_0 hc^3} E_0^2 \sum_{M'} |\langle v'LM' | Q_{\epsilon_0\epsilon}^S(0,\omega) | vLM \rangle + \langle v'LM' | Q_{\epsilon_0\epsilon}^A(0,\omega) | vLM \rangle|^2 \\ &= \frac{2\omega^3}{3\epsilon_0 hc^3} \frac{E_0^2}{2} \sum_{M',q} |\langle v'LM' | Q_{-1q}^S | vLM \rangle + \langle v'LM' | Q_{1q}^S | vLM \rangle \\ &\quad + \langle v'LM' | Q_{-1q}^A | vLM \rangle + \langle v'LM' | Q_{1q}^A | vLM \rangle|^2 \\ &= \frac{\omega^3}{3\epsilon_0 hc^3} E_0^2 \left\{ \frac{3}{2} \left( |\langle LM22 | LM+2 \rangle|^2 + |\langle LM2-2 | LM-2 \rangle|^2 \right) Q_t^2 \right. \\ &\quad + \left| \frac{\sqrt{3}}{2} \langle LM21 | LM+1 \rangle Q_t - \langle LM11 | LM+1 \rangle Q_v \right|^2 \\ &\quad + \left| \frac{\sqrt{3}}{2} \langle LM2-1 | LM-1 \rangle Q_t + \langle LM1-1 | LM-1 \rangle Q_v \right|^2 \\ &\quad + \left| -Q_s + \frac{1}{2} \langle LM20 | LM \rangle Q_t + \langle LM10 | LM \rangle Q_v \right|^2 \\ &\quad \left. + \left| -Q_s + \frac{1}{2} \langle LM20 | LM \rangle Q_t - \langle LM10 | LM \rangle Q_v \right|^2 \right\} \end{aligned} \quad (28)$$

The averaged decay rate is

$$\bar{A}_{v,L,v',L} = \frac{\omega^3}{3\epsilon_0 hc^3} E_0^2 \left( 2Q_s^2 + Q_t^2 + \frac{4}{3} Q_v^2 \right). \quad (29)$$

## II. NUMERICAL METHOD

We now present the calculation of two-photon reduced matrix elements. Our numerical method has been previously described in Refs. [5, 35, 36], and we briefly recall the main points here. The three-body Schröd-

ger equation is solved using the following variational expansion of the wave function :

$$\begin{aligned}\Psi_{LM}(\mathbf{r}_1, \mathbf{r}_2) &= \sum_{l_1+l_2=L} \mathcal{Y}_{LM}^{l_1 l_2}(\mathbf{r}_1, \mathbf{r}_2) R_{l_1 l_2}^L(r_1, r_2, r_{12}), \\ R_{l_1 l_2}^L(r_1, r_2, r_{12}) &= \sum_{n=1}^{N_{l_1}} \left\{ C_n \operatorname{Re} [e^{-\alpha_n r_{12} - \beta_n r_1 - \gamma_n r_2}] + D_n \operatorname{Im} [e^{-\alpha_n r_{12} - \beta_n r_1 - \gamma_n r_2}] \right\}.\end{aligned}\quad (30)$$

$r_1, r_2, r_{12}$  are the interparticle distances, and  $\mathcal{Y}_{LM}^{l_1 l_2}(\mathbf{r}_1, \mathbf{r}_2) = r_1^{l_1} r_2^{l_2} Y_{LM}^{l_1 l_2}(\hat{\mathbf{r}}_1, \hat{\mathbf{r}}_2)$  where  $Y_{LM}^{l_1 l_2}$  is a bipolar spherical harmonic. The complex exponents  $\alpha_n, \beta_n, \gamma_n$  are generated pseudorandomly in several intervals. All parameters, i.e. interval bounds and the number of basis functions  $N_{i, l_1}$  in each interval  $i$  and angular momentum subset  $\{l_1, l_2\}$  (keeping the total basis length  $N = 2 \sum_{i, l_1} N_{i, l_1}$  constant), have been optimized for a few tens of states. This yielded accuracies of  $10^{-12}$  a.u. or better on the energy levels of all 201 rovibrational levels considered here using basis lengths  $N = 2000 - 3500$ .

For the calculation of two-photon matrix elements, the following three terms, which correspond to the possible values  $L'-1, L'+1, L'$  for the angular momentum of the intermediate state, are evaluated numerically :

$$a_{0, \pm} = \frac{1}{\sqrt{(2L+1)(2L'+1)}} \left[ \langle v' L' | \mathbf{d} (E_{vL} - H_{L'})^{-1} \mathbf{d} | v L \rangle + \langle v' L' | \mathbf{d} (E_{v'L'} - H_{L'})^{-1} \mathbf{d} | v L \rangle \right] \quad (31)$$

where  $H_{L''}$  denotes the restriction of the Schrödinger Hamiltonian  $H$  to a subspace of angular momentum  $L''$ , and  $a_0, a_+, a_-$  respectively correspond to  $L'' = L', L'+1, L'-1$ . Basis lengths  $N_{L''} = 2000 - 3000$  are typically used for  $H_{L''}$  which is more than sufficient to obtain these quantities with five significant digits. The reduced matrix elements of  $Q^{(k)}$  are related to  $a_-, a_+, a_0$  in the following way :

$$\frac{\langle v' L \| Q^{(0)} \| v L \rangle}{\sqrt{2L+1}} = \frac{1}{3} (a_- + a_0 + a_+) \quad (32)$$

$$\frac{\langle v' L \| Q^{(1)} \| v L \rangle}{\sqrt{2L+1}} = \sqrt{L(L+1)} \left[ \frac{a_-}{L} + \frac{a_0}{L(L+1)} - \frac{a_+}{L+1} \right] \quad (33)$$

$$\frac{\langle v' L+2 \| Q^{(2)} \| v L \rangle}{\sqrt{2L+5}} = -\sqrt{\frac{2(2L+1)}{3(2L+3)}} a_- \quad (34)$$

$$\frac{\langle v' L \| Q^{(2)} \| v L \rangle}{\sqrt{2L+1}} = -\frac{1}{3} \sqrt{(2L+3)(2L-1)L(L+1)} \left[ \frac{a_-}{L(2L-1)} - \frac{a_0}{L(L+1)} + \frac{a_+}{(2L+3)(L+1)} \right] \quad (35)$$

$$\frac{\langle v' L-2 \| Q^{(2)} \| v L \rangle}{\sqrt{2L-3}} = -\sqrt{\frac{2(2L+1)}{3(2L-1)}} a_+ \quad (36)$$

### III. RESULTS AND DISCUSSION

The range of ro-vibrational states was chosen in order to provide all the results relevant to any of the following experimental situations :

- (i)  $\text{H}_2^+$  ions produced by electron-impact ionization of  $\text{H}_2$ . This process has been shown to create ions predominantly in  $v = 0 - 12, L = 0 - 4$  with only  $\sim 1$  percent probability of populating higher vibrational states [37].
- (ii)  $\bar{\text{H}}_2^-$  antimatter ions produced through the reaction  $\bar{\text{H}}^+ + \bar{p} \rightarrow \bar{\text{H}}_2^- + e^+$ , as proposed in [12], using  $\bar{\text{H}}^+$  ions to be produced in the GBAR experiment [38]. The reaction being exothermic by 1.896 eV, the  $\bar{\text{H}}_2^-$  ion will be produced with  $v = 0 - 8$  and  $L = 0 - 27$ , with low- $v$ , high  $L$  states being favored.

The two-photon matrix elements  $Q_s, Q_v$  and  $Q_t$  were calculated for all the required states [39]. The corresponding  $M$ -averaged decay rates  $A/(B_0^4 r_c^2)$  in  $\text{s}^{-1} \text{T}^{-4} \text{mm}^{-2}$  are given in the following Tables for  $L \rightarrow L' = L-2$  ( $\Delta v = v - v' = 0, 1, 2$ , Tables I-III),  $L \rightarrow L' = L$  ( $\Delta v = 1, 2$ , Tables IV-V), and  $L \rightarrow L' = L+2$  transitions ( $\Delta v = 1, 2$ , Tables VI-VII). The total decay rates  $\bar{A}_{v,L} = \sum_{v', L'} \bar{A}_{v, L, v', L'}$  are given in Table VIII.

The decay rates decrease sharply with increasing  $\Delta v$ , as previously observed in the case of two-photon transitions [40]. Decay towards  $v' = v - 3$  states was also included in the total rates of Table VIII. However, since the fractional contribution of  $\Delta v = 3$  transitions to the overall decay rates amounts to less than  $10^{-3}$  in all cases, these decay rates are not reported here.

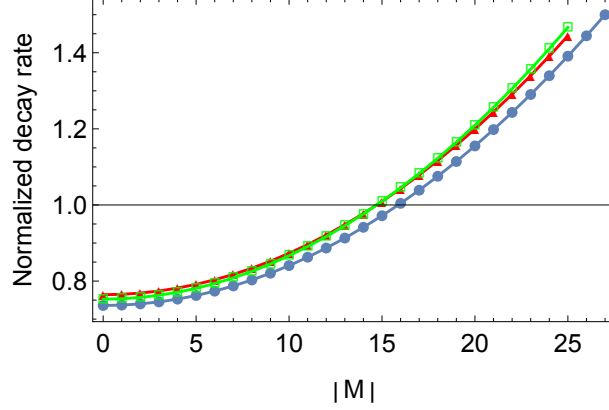


FIGURE 1: Normalized decay rate  $A_{v,L,M,v',L'}/\bar{A}_{v,L,v',L'}$  for  $L = 27, L' = 25$  (blue circles),  $L = 25, L' = 27$  (red triangles), and  $v = 1, L = 25, v' = 0, L' = 25$  (green squares). Note that the  $M$  dependence is independent of  $v$  and  $v'$  for  $\Delta L = \pm 2$  (see Eq. (26)), but not for  $\Delta L = 0$  (Eq. (28)).

The dependence of the decay rates on the magnetic quantum number  $M$  is illustrated in Fig. 1. One can see that the decay rate increases with  $|M|$ .

These results can be used to precisely model the time evolution of  $H_2^+$  (or  $\bar{H}_2^-$ ) ro-vibrational populations from initial conditions corresponding to different production schemes. Such a study is outside the scope of the present paper, but it is already possible to draw some qualitative conclusions. Fig. 2 shows both zero-field and Stark-quenched lifetimes of selected ro-vibrational states, for a magnetic field value  $B_0 = 8.5$  T and a cyclotron radius  $r_c = 2$  mm which correspond to the parameters of the Penning trap operated in Tallahassee [41].

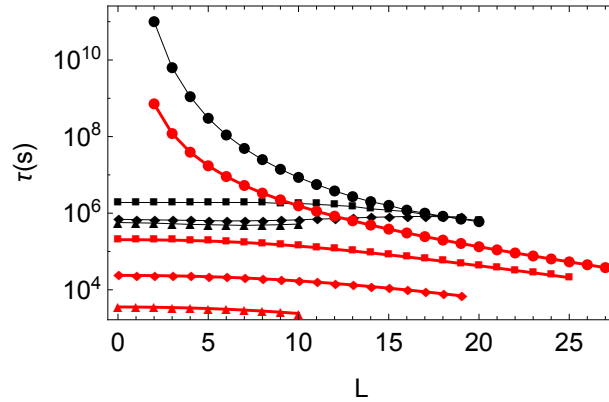


FIGURE 2: Stark lifetimes of  $H_2^+$  rovibrational states for an ion in a cyclotron orbit of radius  $r_c = 2$  mm in a magnetic field  $B_0 = 8.5$  T are shown by thick red lines. For comparison, the zero-field lifetimes (taken from [24]) are shown by thin black lines. Circles, squares, diamonds and triangles respectively stand for  $v = 0, 1, 4, 8$ .

One may observe that Stark quenching is most efficient for excited vibrational states, leading to lifetimes of e.g. less than one hour for  $v = 8$ , a few hours for  $v = 4$ , and a few days for  $v = 1$ . This represents a reduction by 1-2 orders of magnitude with respect to the zero-field lifetime. Quenching of the vibrational motion down to  $v = 0$  may thus be expected to occur within  $\sim 1$  week in present-day Penning traps. Quenching of the rotational motion is significantly slower, with lifetimes ranging from  $\sim 10$  hours for ( $v = 0, L = 27$ ) up to  $\sim 23$  years for ( $v = 0, L = 2$ ). Thus for manipulation of antimatter molecular ions which may be formed in high- $L$  states [12] it would be useful to transfer the ions to a larger trap where the ions could be placed in a cyclotron orbit of very large radius. For example, for  $B_0 = 10$  T and  $r_c = 20$  mm, the lifetimes would range from  $\sim 3$  minutes for ( $v = 0, L = 27$ ) to  $\sim 7$  days for ( $v = 0, L = 3$ ). Rotational quenching down to  $L = 1$  or 2 could thus occur in about 1 week.

In conclusion, our results indicate that vibrational quenching of  $H_2^+$  or its antimatter counterpart may be achieved within  $\sim 1$  week in existing Penning trap apparatus, and that rotational quenching is achievable

over a similar time scale in a specially designed apparatus allowing for larger cyclotron radii. This opens new possibilities for ultra-high resolution spectroscopy of the simplest (anti)-molecule. Rovibrational Stark quenching of  $\text{H}_2^+$  (and other homonuclear diatomic molecular ions) could also be significant if they are stored in heavy-ion storage rings in which the bending sections have comparably large values of  $B_0^4 r_c^2$ .

Finally, it is worth noting that, although we have focused on the case of an  $\text{H}_2^+$  ion orbiting in an external magnetic field, the results presented here may readily be applied to calculate its decay rates in an external static electric field  $\mathbf{E}_0$ . Since the decay rate of a particular  $M$  state depends on the electric field polarization, Eqs. (26) and (28) have to be adapted to the specific case under study. However, the averaged decay rates are independent of the field polarization, so that Eqs. (25), (27), and (29) may be directly applied. The results of Tables I-VIII can also be directly exploited using the relationship  $E_0 = qB_0^2 r_c / m$ .

### Acknowledgments

I thank E.G. Myers for bringing this problem to my attention and for stimulating discussions. I also thank him, as well as L. Hilico, for useful suggestions on the manuscript. I acknowledge support as a fellow of the Institut Universitaire de France.

- 
- [1] W.H. Wing, G.A. Ruff, W.E. Lamb, Jr., and J.J. Spezeski, *Phys. Rev. Lett.* **36**, 1488 (1976).
  - [2] B. Roth, J. Koelemeij, S. Schiller, L. Hilico, J.-Ph. Karr, V. I. Korobov, and D. Bakalov, *Precision Physics of Simple Atoms and Molecules*, ed. S. Karshenboim, *Lectures Notes in Physics* **745**, 205. (Springer-Verlag, Berlin, Heidelberg, 2008).
  - [3] S. Schiller and V Korobov, *Phys. Rev. A* **71**, 032505 (2005).
  - [4] S. Schiller, D. Bakalov, and V.I. Korobov, *Phys. Rev. Lett.* **113**, 023004 (2014).
  - [5] J.-Ph. Karr, *J. Mol. Spectrosc.* **300**, 37 (2014).
  - [6] J.-Ph. Karr, L. Hilico, J. C. J. Koelemeij, V.I. Korobov, *Phys. Rev. A* **94**, 050501(R) (2016).
  - [7] A. Antognini *et al.*, *Science* **339**, 417 (2013).
  - [8] J. Arrington and I. Sick, *J. Phys. Chem. Ref. Data* **44**, 031204 (2015).
  - [9] R. Pohl *et al.*, *Science* **353**, 669 (2016).
  - [10] A. Beyer *et al.*, *Science* **358**, 79 (2017).
  - [11] H. Fleurbaey, S. Galtier, S. Thomas, M. Bonnaud, L. Julien, F. Biraben, F. Nez, M. Abgrall, and J. Guéna, *Phys. Rev. Lett.* **120**, 183001 (2018).
  - [12] E.G. Myers, *Phys. Rev. A* **98**, 010101 (2018).
  - [13] V. I. Korobov, L. Hilico, J.-Ph. Karr, *Phys. Rev. Lett.* **118**, 233001 (2017).
  - [14] S. Sturm, F. Köhler, J. Zatorski, A. Wagner, Z. Harman, G. Werth, W. Quint, C.H. Keitel, and K. Blaum, *Nature* **467**, 506 (2014).
  - [15] F. Heiße, F. Köhler-Langes, S. Rau, J. Hou, S. Junck, A. Kracke, A. Mooser, W. Quint, S. Ulmer, G. Werth, K. Blaum, S. Sturm, *Phys. Rev. Lett.* **119**, 033001 (2017).
  - [16] U. Bressel, A. Borodin, J. Shen, M. Hansen, I. Ernsting, and S. Schiller, *Phys. Rev. Lett.* **108**, 183003 (2012).
  - [17] J. Biesheuvel, J.-Ph. Karr, L. Hilico, K.S.E. Eikema, W. Ubachs, and J.C.J. Koelemeij, *Nature Comm.* **7**, 10385 (2016).
  - [18] S. Alighanbari, M.G. Hansen, V.I. Korobov, and S. Schiller, *Nat. Phys.* **14**, 555 (2018).
  - [19] K.B. Jefferts, *Phys. Rev. Lett.* **23**, 1476 (1969).
  - [20] A. Carrington, C.A. Leach, R.E. Moss, T.C. Steimle, M.R. Viant, and Y.D. West, *J. Chem. Soc. Faraday Trans.* **89**, 603 (1993).
  - [21] A.D.J. Critchley, A.N. Hughes, and I.R. McNab, *Phys. Rev. Lett.* **86**, 1725 (2001).
  - [22] C. Haase, M. Beyer, C. Jungen, and F. Merkt, *J. Chem. Phys.* **142**, 064310 (2015).
  - [23] M. Beyer and F. Merkt, *Phys. Rev. Lett.* **116**, 093001 (2016).
  - [24] A.G. Posen, A. Dalgarno, and J.M. Peek, *At. Data and Nucl. Data Tables* **28**, 265 (1983).
  - [25] H. Olivares Pilón and D. Baye, *J. Phys. B* **45**, 065101 (2012).
  - [26] T. Schneider, B. Roth, H. Duncker, I. Ernsting, and S. Schiller, *Nature Phys.* **6**, 275 (2010).
  - [27] J.-Ph. Karr, A. Douillet, and L. Hilico, *Appl. Phys. B* **107**, 1043 (2012).
  - [28] S.L. Anderson, G.D. Kubiak, and R.N. Zare, *Chem. Phys. Lett.* **105**, 22 (1984).
  - [29] M.A. O'Halloran, S.T. Pratt, P.M. Dehmer, and J.L. Dehmer, *J. Chem. Phys.* **87**, 3288 (1987).
  - [30] S. Schiller, I. Kortunov, M. Hernández Vera, F. Gianturco, and H. da Silva, Jr., *Phys. Rev. A* **95**, 043411 (2017).
  - [31] J.K. Thompson, S. Rainville, and D.E. Pritchard, *Nature* **430**, 58 (2004).
  - [32] W.E. Lamb and R.C. Retherford, *Phys. Rev.* **79**, 549 (1950).
  - [33] G. Grynberg, *Habilitation thesis, Université Pierre et Marie Curie (Paris 6)* (1976).
  - [34] G. Grynberg, F. Biraben, E. Giacobino, and B. Cagnac, *J. Phys.* **38**, 629 (1977).

- [35] J.-Ph. Karr, F. Bielsa, A. Douillet, J. Pedregosa Gutierrez, V.I. Korobov, and L. Hilico, Phys. Rev. A **77**, 063410 (2008).
- [36] V.I. Korobov, Mol. Phys. **116**, 93 (2017).
- [37] F. von Busch and G.H. Dunn, Phys. Rev. A **5**, 1726 (1972).
- [38] P. Perez *et al.*, Hyperfine Interact. **233**, 21 (2015).
- [39] See Supplemental Material at ... for the values of the two-photon matrix elements.
- [40] L. Hilico, N. Billy, B. Grémaud, and D. Delande, J. Phys. B **34**, 1 (2001).
- [41] J.A. Smith, S. Hamzeloui, D.J. Fink, and E.G. Myers, Phys. Rev. Lett. **120**, 143002 (2018).



TABLE I: Averaged decay rates  $\bar{A}_{v,L,v',L'}/(B_0^4 r_c^2)$  in  $\text{s}^{-1}\text{T}^{-4}\text{mm}^{-2}$  with  $v' = v$ ,  $L' = L - 2$ .

$L/v$	0	1	2	3	4	5	6	7	8	9	10	11	12
2	6.693E-14	1.154E-13	1.911E-13	3.085E-13	4.896E-13	7.703E-13	1.209E-12	1.904E-12	3.029E-12	4.900E-12	8.124E-12	1.395E-11	2.517E-11
3	3.996E-13	6.882E-13	1.139E-12	1.838E-12	2.918E-12	4.591E-12	7.207E-12	1.136E-11	1.808E-11	2.928E-11	4.861E-11	8.366E-11	
4	1.224E-12	2.105E-12	3.482E-12	5.615E-12	8.912E-12	1.402E-11	2.203E-11	3.474E-11	5.537E-11	8.981E-11	1.495E-10	2.580E-10	
5	2.774E-12	4.765E-12	7.875E-12	1.269E-11	2.014E-11	3.170E-11	4.983E-11	7.868E-11	1.256E-10	2.042E-10	3.409E-10		
6	5.299E-12	9.084E-12	1.500E-11	2.416E-11	3.833E-11	6.035E-11	9.494E-11	1.501E-10	2.402E-10	3.916E-10	6.564E-10		
7	9.062E-12	1.550E-11	2.556E-11	4.114E-11	6.527E-11	1.028E-10	1.620E-10	2.566E-10	4.116E-10	6.735E-10			
8	1.435E-11	2.448E-11	4.031E-11	6.485E-11	1.029E-10	1.623E-10	2.559E-10	4.064E-10	6.539E-10	1.075E-09			
9	2.146E-11	3.653E-11	6.007E-11	9.660E-11	1.533E-10	2.420E-10	3.824E-10	6.089E-10	9.836E-10				
10	3.075E-11	5.221E-11	8.574E-11	1.378E-10	2.189E-10	3.459E-10	5.479E-10	8.752E-10	1.420E-09				
11	4.259E-11	7.214E-11	1.183E-10	1.902E-10	3.022E-10	4.785E-10	7.599E-10	1.219E-09					
12	5.741E-11	9.703E-11	1.590E-10	2.555E-10	4.066E-10	6.451E-10	1.028E-09	1.656E-09					
13	7.569E-11	1.277E-10	2.090E-10	3.361E-10	5.355E-10	8.519E-10	1.363E-09						
14	9.800E-11	1.650E-10	2.700E-10	4.345E-10	6.936E-10	1.107E-09	1.779E-09						
15	1.250E-10	2.101E-10	3.437E-10	5.538E-10	8.862E-10	1.420E-09							
16	1.573E-10	2.641E-10	4.323E-10	6.977E-10	1.120E-09	1.802E-09							
17	1.959E-10	3.287E-10	5.384E-10	8.708E-10	1.403E-09	2.270E-09							
18	2.417E-10	4.055E-10	6.651E-10	1.079E-09	1.746E-09								
19	2.959E-10	4.965E-10	8.161E-10	1.328E-09	2.161E-09								
20	3.599E-10	6.044E-10	9.959E-10	1.628E-09									
21	4.352E-10	7.320E-10	1.210E-09	1.989E-09									
22	5.238E-10	8.831E-10	1.466E-09										
23	6.279E-10	1.062E-09	1.772E-09										
24	7.503E-10	1.274E-09											
25	8.942E-10	1.526E-09											
26	1.064E-09												
27	1.264E-09												

TABLE II: Same as Table I, with  $v' = v - 1$ .

$L/v$	1	2	3	4	5	6	7	8	9	10	11	12
2	2.819E-11	7.437E-11	1.476E-10	2.618E-10	4.384E-10	7.110E-10	1.134E-09	1.798E-09	2.857E-09	4.584E-09	7.489E-09	1.259E-08
3	3.959E-11	1.042E-10	2.066E-10	3.659E-10	6.122E-10	9.926E-10	1.583E-09	2.511E-09	3.990E-09	6.408E-09	1.048E-08	
4	4.789E-11	1.258E-10	2.489E-10	4.404E-10	7.362E-10	1.193E-09	1.903E-09	3.019E-09	4.802E-09	7.721E-09	1.266E-08	
5	5.512E-11	1.445E-10	2.855E-10	5.044E-10	8.426E-10	1.365E-09	2.177E-09	3.455E-09	5.502E-09	8.860E-09		
6	6.198E-11	1.621E-10	3.197E-10	5.643E-10	9.418E-10	1.525E-09	2.434E-09	3.865E-09	6.162E-09	9.943E-09		
7	6.876E-11	1.794E-10	3.533E-10	6.228E-10	1.039E-09	1.682E-09	2.685E-09	4.269E-09	6.817E-09			
8	7.564E-11	1.970E-10	3.871E-10	6.818E-10	1.137E-09	1.841E-09	2.940E-09	4.680E-09	7.488E-09			
9	8.274E-11	2.150E-10	4.219E-10	7.424E-10	1.237E-09	2.004E-09	3.204E-09	5.108E-09				
10	9.016E-11	2.338E-10	4.582E-10	8.056E-10	1.343E-09	2.176E-09	3.482E-09	5.562E-09				
11	9.800E-11	2.537E-10	4.965E-10	8.725E-10	1.454E-09	2.359E-09	3.780E-09					
12	1.063E-10	2.748E-10	5.374E-10	9.440E-10	1.574E-09	2.555E-09	4.103E-09					
13	1.153E-10	2.975E-10	5.814E-10	1.021E-09	1.704E-09	2.770E-09						
14	1.250E-10	3.221E-10	6.291E-10	1.105E-09	1.845E-09	3.005E-09						
15	1.355E-10	3.489E-10	6.812E-10	1.197E-09	2.002E-09							
16	1.470E-10	3.782E-10	7.386E-10	1.299E-09	2.176E-09							
17	1.596E-10	4.105E-10	8.021E-10	1.413E-09	2.370E-09							
18	1.735E-10	4.463E-10	8.727E-10	1.539E-09								
19	1.889E-10	4.862E-10	9.516E-10	1.681E-09								
20	2.060E-10	5.307E-10	1.040E-09									
21	2.252E-10	5.806E-10	1.140E-09									
22	2.466E-10	6.368E-10										
23	2.708E-10	7.003E-10										
24	2.980E-10											
25	3.288E-10											

TABLE III: Same as Table I, with  $v' = v - 2$ .

$L/v$	2	3	4	5	6	7	8	9	10	11	12
2	1.874E-12	6.880E-12	1.704E-11	3.562E-11	6.787E-11	1.223E-10	2.129E-10	3.628E-10	6.114E-10	1.028E-09	1.739E-09
3	2.072E-12	7.608E-12	1.886E-11	3.945E-11	7.522E-11	1.356E-10	2.362E-10	4.024E-10	6.777E-10	1.138E-09	
4	1.958E-12	7.197E-12	1.786E-11	3.741E-11	7.143E-11	1.290E-10	2.247E-10	3.829E-10	6.445E-10	1.080E-09	
5	1.745E-12	6.426E-12	1.598E-11	3.355E-11	6.418E-11	1.160E-10	2.024E-10	3.451E-10	5.804E-10		
6	1.503E-12	5.550E-12	1.385E-11	2.915E-11	5.591E-11	1.013E-10	1.770E-10	3.018E-10	5.073E-10		
7	1.260E-12	4.674E-12	1.171E-11	2.475E-11	4.764E-11	8.657E-11	1.515E-10	2.584E-10			
8	1.032E-12	3.849E-12	9.697E-12	2.060E-11	3.983E-11	7.262E-11	1.273E-10	2.172E-10			
9	8.236E-13	3.097E-12	7.863E-12	1.682E-11	3.269E-11	5.984E-11	1.051E-10				
10	6.392E-13	2.430E-12	6.231E-12	1.344E-11	2.630E-11	4.836E-11	8.507E-11				
11	4.797E-13	1.851E-12	4.807E-12	1.048E-11	2.068E-11	3.819E-11					
12	3.447E-13	1.358E-12	3.587E-12	7.929E-12	1.579E-11	2.931E-11					
13	2.337E-13	9.471E-13	2.562E-12	5.763E-12	1.161E-11						
14	1.455E-13	6.154E-13	1.721E-12	3.963E-12	8.096E-12						
15	7.890E-14	3.581E-13	1.053E-12	2.508E-12							
16	3.296E-14	1.715E-13	5.512E-13	1.384E-12							
17	6.870E-15	5.313E-14	2.096E-13	5.839E-13							
18	2.459E-16	2.122E-15	2.878E-14								
19	1.320E-14	1.988E-14	1.580E-14								
20	4.654E-14	1.108E-13									
21	1.019E-13	2.832E-13									
22	1.822E-13										
23	2.917E-13										

TABLE IV: Averaged decay rates  $\bar{A}_{v,L,v',L'}/(B_0^4 r_c^2)$  in  $\text{s}^{-1}\text{T}^{-4}\text{mm}^{-2}$  with  $v' = v - 1$ ,  $L' = L$ .

$L/v$	1	2	3	4	5	6	7	8	9	10	11	12
0	1.298E-10	3.033E-10	5.405E-10	8.716E-10	1.343E-09	2.027E-09	3.040E-09	4.576E-09	6.963E-09	1.079E-08	1.713E-08	2.816E-08
1	1.794E-10	4.344E-10	8.014E-10	1.335E-09	2.120E-09	3.289E-09	5.055E-09	7.771E-09	1.204E-08	1.893E-08	3.044E-08	5.052E-08
2	1.665E-10	4.003E-10	7.335E-10	1.215E-09	1.918E-09	2.962E-09	4.536E-09	6.952E-09	1.075E-08	1.688E-08	2.713E-08	4.505E-08
3	1.659E-10	3.986E-10	7.301E-10	1.209E-09	1.909E-09	2.948E-09	4.516E-09	6.928E-09	1.072E-08	1.687E-08	2.717E-08	
4	1.673E-10	4.024E-10	7.376E-10	1.222E-09	1.932E-09	2.988E-09	4.584E-09	7.045E-09	1.093E-08	1.723E-08	2.785E-08	
5	1.698E-10	4.089E-10	7.506E-10	1.246E-09	1.973E-09	3.056E-09	4.699E-09	7.239E-09	1.126E-08	1.782E-08		
6	1.731E-10	4.175E-10	7.678E-10	1.277E-09	2.026E-09	3.147E-09	4.852E-09	7.497E-09	1.170E-08	1.860E-08		
7	1.771E-10	4.281E-10	7.891E-10	1.315E-09	2.093E-09	3.260E-09	5.041E-09	7.819E-09	1.226E-08			
8	1.819E-10	4.407E-10	8.144E-10	1.361E-09	2.172E-09	3.395E-09	5.270E-09	8.209E-09	1.294E-08			
9	1.874E-10	4.553E-10	8.438E-10	1.415E-09	2.266E-09	3.554E-09	5.541E-09	8.673E-09				
10	1.937E-10	4.721E-10	8.778E-10	1.477E-09	2.375E-09	3.741E-09	5.860E-09	9.223E-09				
11	2.008E-10	4.911E-10	9.165E-10	1.548E-09	2.500E-09	3.957E-09	6.232E-09					
12	2.089E-10	5.127E-10	9.606E-10	1.630E-09	2.644E-09	4.207E-09	6.666E-09					
13	2.179E-10	5.370E-10	1.010E-09	1.722E-09	2.809E-09	4.496E-09						
14	2.280E-10	5.643E-10	1.067E-09	1.828E-09	2.998E-09	4.829E-09						
15	2.392E-10	5.949E-10	1.131E-09	1.948E-09	3.214E-09							
16	2.517E-10	6.292E-10	1.202E-09	2.084E-09	3.462E-09							
17	2.657E-10	6.677E-10	1.283E-09	2.239E-09	3.748E-09							
18	2.812E-10	7.109E-10	1.375E-09	2.416E-09								
19	2.985E-10	7.594E-10	1.479E-09	2.619E-09								
20	3.178E-10	8.139E-10	1.597E-09									
21	3.394E-10	8.754E-10	1.731E-09									
22	3.636E-10	9.449E-10										
23	3.907E-10	1.024E-09										
24	4.211E-10											
25	4.554E-10											

TABLE V: Same as Table IV, with  $v' = v - 2$ .

$L/v$	2	3	4	5	6	7	8	9	10	11	12
0	1.717E-12	7.717E-12	2.265E-11	5.468E-11	1.178E-10	2.360E-10	4.500E-10	8.297E-10	1.497E-09	2.669E-09	4.748E-09
1	6.366E-12	2.480E-11	6.501E-11	1.433E-10	2.867E-10	5.404E-10	9.804E-10	1.735E-09	3.026E-09	5.249E-09	9.135E-09
2	5.116E-12	2.024E-11	5.376E-11	1.199E-10	2.424E-10	4.613E-10	8.435E-10	1.503E-09	2.638E-09	4.600E-09	8.045E-09
3	5.001E-12	1.985E-11	5.291E-11	1.183E-10	2.399E-10	4.574E-10	8.381E-10	1.497E-09	2.631E-09	4.597E-09	
4	5.063E-12	2.013E-11	5.374E-11	1.203E-10	2.443E-10	4.664E-10	8.558E-10	1.530E-09	2.694E-09	4.716E-09	
5	5.207E-12	2.073E-11	5.539E-11	1.242E-10	2.523E-10	4.823E-10	8.858E-10	1.586E-09	2.797E-09		
6	5.412E-12	2.157E-11	5.768E-11	1.294E-10	2.632E-10	5.037E-10	9.263E-10	1.661E-09	2.934E-09		
7	5.673E-12	2.263E-11	6.057E-11	1.360E-10	2.770E-10	5.306E-10	9.771E-10	1.755E-09			
8	5.992E-12	2.392E-11	6.410E-11	1.441E-10	2.937E-10	5.633E-10	1.039E-09	1.869E-09			
9	6.373E-12	2.547E-11	6.830E-11	1.537E-10	3.136E-10	6.024E-10	1.113E-09				
10	6.823E-12	2.729E-11	7.327E-11	1.651E-10	3.373E-10	6.488E-10	1.201E-09				
11	7.350E-12	2.943E-11	7.909E-11	1.784E-10	3.650E-10	7.034E-10					
12	7.964E-12	3.192E-11	8.589E-11	1.940E-10	3.976E-10	7.676E-10					
13	8.677E-12	3.482E-11	9.381E-11	2.122E-10	4.356E-10						
14	9.504E-12	3.819E-11	1.030E-10	2.334E-10	4.800E-10						
15	1.046E-11	4.209E-11	1.137E-10	2.581E-10							
16	1.157E-11	4.661E-11	1.261E-10	2.868E-10							
17	1.285E-11	5.186E-11	1.406E-10	3.203E-10							
18	1.434E-11	5.796E-11	1.574E-10								
19	1.606E-11	6.503E-11	1.770E-10								
20	1.806E-11	7.327E-11									
21	2.039E-11	8.286E-11									
22	2.309E-11										
23	2.623E-11										

TABLE VI: Averaged decay rates  $\bar{A}_{v,L,v',L'}/(B_0^4 r_c^2)$  in  $\text{s}^{-1}\text{T}^{-4}\text{mm}^{-2}$  with  $v' = v - 1$ ,  $L' = L + 2$ . Stars indicate cases where the  $(v - 1, L + 2)$  level lies above the  $(v, L)$  level. In these cases, the "reversed" decay rate  $\bar{A}_{v',L',v,L}/(B_0^4 r_c^2)$  is given instead.

$L/v$	1	2	3	4	5	6	7	8	9	10	11	12
0	1.056E-10	2.798E-10	5.574E-10	9.913E-10	1.663E-09	2.701E-09	4.312E-09	6.835E-09	1.085E-08	1.739E-08	2.835E-08	4.750E-08
1	5.695E-11	1.511E-10	3.013E-10	5.362E-10	9.001E-10	1.462E-09	2.335E-09	3.701E-09	5.875E-09	9.412E-09	1.534E-08	2.570E-08
2	4.364E-11	1.159E-10	2.312E-10	4.117E-10	6.913E-10	1.123E-09	1.794E-09	2.843E-09	4.513E-09	7.230E-09	1.178E-08	1.974E-08
3	3.590E-11	9.539E-11	1.904E-10	3.391E-10	5.695E-10	9.255E-10	1.478E-09	2.342E-09	3.717E-09	5.953E-09	9.702E-09	
4	3.024E-11	8.036E-11	1.604E-10	2.857E-10	4.798E-10	7.796E-10	1.244E-09	1.972E-09	3.129E-09	5.009E-09	8.162E-09	
5	2.566E-11	6.820E-11	1.361E-10	2.424E-10	4.069E-10	6.609E-10	1.054E-09	1.670E-09	2.648E-09	4.237E-09		
6	2.179E-11	5.788E-11	1.155E-10	2.055E-10	3.448E-10	5.596E-10	8.921E-10	1.412E-09	2.236E-09	3.573E-09		
7	1.843E-11	4.891E-11	9.751E-11	1.734E-10	2.905E-10	4.710E-10	7.499E-10	1.185E-09	1.874E-09			
8	1.548E-11	4.103E-11	8.170E-11	1.450E-10	2.427E-10	3.928E-10	6.240E-10	9.837E-10	1.551E-09			
9	1.288E-11	3.408E-11	6.772E-11	1.200E-10	2.003E-10	3.234E-10	5.123E-10	8.046E-10				
10	1.058E-11	2.794E-11	5.539E-11	9.787E-11	1.629E-10	2.619E-10	4.131E-10	6.454E-10				
11	8.568E-12	2.255E-11	4.455E-11	7.840E-11	1.299E-10	2.078E-10	3.256E-10					
12	6.809E-12	1.785E-11	3.509E-11	6.142E-11	1.011E-10	1.605E-10	2.491E-10					
13	5.288E-12	1.378E-11	2.692E-11	4.676E-11	7.627E-11	1.197E-10						
14	3.990E-12	1.032E-11	1.997E-11	3.432E-11	5.523E-11	8.525E-11						
15	2.901E-12	7.421E-12	1.418E-11	2.398E-11	3.784E-11							
16	2.010E-12	5.061E-12	9.489E-12	1.567E-11	2.399E-11							
17	1.303E-12	3.207E-12	5.841E-12	9.294E-12	1.353E-11							
18	7.696E-13	1.826E-12	3.172E-12	4.739E-12								
19	3.939E-13	8.781E-13	1.402E-12	1.858E-12								
20	1.583E-13	3.124E-13	4.173E-13									
21	3.880E-14	5.593E-14	4.244E-14									
22	1.911E-15	2.881E-16										
23	9.695E-16*	1.756E-14*										
24	3.659E-14*											
25	1.999E-13*											

TABLE VII: Same as Table VI, with  $v' = v - 2$ .

$L/v$	2	3	4	5	6	7	8	9	10	11	12
0	1.392E-11	5.119E-11	1.269E-10	2.654E-10	5.057E-10	9.117E-10	1.588E-09	2.712E-09	4.587E-09	7.753E-09	1.322E-08
1	9.373E-12	3.450E-11	8.562E-11	1.792E-10	3.417E-10	6.165E-10	1.075E-09	1.838E-09	3.114E-09	5.275E-09	9.023E-09
2	8.947E-12	3.298E-11	8.194E-11	1.717E-10	3.277E-10	5.918E-10	1.033E-09	1.769E-09	3.003E-09	5.102E-09	8.759E-09
3	9.163E-12	3.383E-11	8.416E-11	1.765E-10	3.374E-10	6.102E-10	1.067E-09	1.830E-09	3.115E-09	5.307E-09	
4	9.614E-12	3.555E-11	8.858E-11	1.861E-10	3.561E-10	6.451E-10	1.130E-09	1.943E-09	3.315E-09	5.668E-09	
5	1.018E-11	3.772E-11	9.415E-11	1.981E-10	3.798E-10	6.891E-10	1.210E-09	2.085E-09	3.568E-09		
6	1.083E-11	4.018E-11	1.004E-10	2.117E-10	4.066E-10	7.393E-10	1.301E-09	2.249E-09	3.862E-09		
7	1.152E-11	4.283E-11	1.073E-10	2.265E-10	4.360E-10	7.945E-10	1.402E-09	2.430E-09			
8	1.225E-11	4.565E-11	1.145E-10	2.424E-10	4.675E-10	8.541E-10	1.511E-09	2.630E-09			
9	1.302E-11	4.860E-11	1.222E-10	2.591E-10	5.011E-10	9.179E-10	1.629E-09				
10	1.382E-11	5.168E-11	1.302E-10	2.768E-10	5.366E-10	9.860E-10	1.756E-09				
11	1.464E-11	5.489E-11	1.386E-10	2.954E-10	5.743E-10	1.059E-09					
12	1.550E-11	5.823E-11	1.474E-10	3.150E-10	6.141E-10	1.136E-09					
13	1.639E-11	6.171E-11	1.566E-10	3.356E-10	6.564E-10						
14	1.732E-11	6.535E-11	1.663E-10	3.573E-10	7.013E-10						
15	1.828E-11	6.915E-11	1.764E-10	3.803E-10							
16	1.928E-11	7.312E-11	1.871E-10	4.046E-10							
17	2.032E-11	7.728E-11	1.983E-10	4.303E-10							
18	2.141E-11	8.165E-11	2.102E-10								
19	2.255E-11	8.622E-11	2.226E-10								
20	2.374E-11	9.101E-11									
21	2.498E-11	9.601E-11									
22	2.626E-11										
23	2.758E-11										

TABLE VIII: Total decay rates  $\bar{A}_{v,L}/(B_0^4 r_c^2)$  in  $\text{s}^{-1}\text{T}^{-4}\text{mm}^{-2}$ .

$L/v$	0	1	2	3	4	5	6	7	8	9	10	11	12
0	0	2.353E-10	5.987E-10	1.157E-09	2.013E-09	3.327E-09	5.354E-09	8.503E-09	1.346E-08	2.136E-08	3.427E-08	5.592E-08	9.367E-08
1	0	2.363E-10	6.013E-10	1.162E-09	2.022E-09	3.343E-09	5.381E-09	8.549E-09	1.353E-08	2.150E-08	3.450E-08	5.633E-08	9.442E-08
2	6.693E-14	2.384E-10	6.067E-10	1.173E-09	2.042E-09	3.377E-09	5.438E-09	8.644E-09	1.369E-08	2.177E-08	3.497E-08	5.717E-08	9.599E-08
3	3.996E-13	2.420E-10	6.156E-10	1.190E-09	2.073E-09	3.430E-09	5.528E-09	8.795E-09	1.395E-08	2.220E-08	3.571E-08	5.850E-08	
4	1.224E-12	2.475E-10	6.286E-10	1.216E-09	2.118E-09	3.507E-09	5.656E-09	9.010E-09	1.431E-08	2.281E-08	3.678E-08	6.041E-08	
5	2.774E-12	2.553E-10	6.466E-10	1.250E-09	2.178E-09	3.610E-09	5.830E-09	9.299E-09	1.479E-08	2.364E-08	3.822E-08		
6	5.299E-12	2.659E-10	6.702E-10	1.295E-09	2.257E-09	3.744E-09	6.054E-09	9.674E-09	1.542E-08	2.471E-08	4.010E-08		
7	9.062E-12	2.798E-10	7.005E-10	1.351E-09	2.357E-09	3.913E-09	6.337E-09	1.015E-08	1.622E-08	2.608E-08			
8	1.435E-11	2.975E-10	7.383E-10	1.422E-09	2.479E-09	4.122E-09	6.687E-09	1.073E-08	1.721E-08	2.778E-08			
9	2.146E-11	3.195E-10	7.847E-10	1.507E-09	2.629E-09	4.376E-09	7.114E-09	1.145E-08	1.843E-08				
10	3.075E-11	3.466E-10	8.408E-10	1.611E-09	2.809E-09	4.682E-09	7.629E-09	1.232E-08	1.991E-08				
11	4.259E-11	3.795E-10	9.081E-10	1.734E-09	3.024E-09	5.048E-09	8.246E-09	1.336E-08					
12	5.741E-11	4.190E-10	9.881E-10	1.880E-09	3.279E-09	5.482E-09	8.982E-09	1.462E-08					
13	7.569E-11	4.661E-10	1.083E-09	2.053E-09	3.580E-09	5.996E-09	9.857E-09						
14	9.800E-11	5.219E-10	1.194E-09	2.255E-09	3.933E-09	6.603E-09	1.090E-08						
15	1.250E-10	5.876E-10	1.324E-09	2.492E-09	4.348E-09	7.318E-09							
16	1.573E-10	6.648E-10	1.476E-09	2.768E-09	4.834E-09	8.162E-09							
17	1.959E-10	7.552E-10	1.653E-09	3.092E-09	5.405E-09	9.159E-09							
18	2.417E-10	8.609E-10	1.860E-09	3.470E-09	6.076E-09								
19	2.959E-10	9.843E-10	2.101E-09	3.912E-09	6.866E-09								
20	3.599E-10	1.128E-09	2.383E-09	4.431E-09									
21	4.352E-10	1.297E-09	2.712E-09	5.040E-09									
22	5.238E-10	1.493E-09	3.097E-09										
23	6.279E-10	1.723E-09	3.550E-09										
24	7.503E-10	1.993E-09											
25	8.942E-10	2.311E-09											
26	1.064E-09												
27	1.264E-09												